

The multichannel nature of three-body recombination for ultracold ^{39}K

T. Secker,* J.-L. Li,* P. M. A. Mestrom, and S. J. J. M. F. Kokkelmans
 Eindhoven University of Technology, P. O. Box 513, 5600 MB Eindhoven, The Netherlands
 (Dated: December 16, 2021)

We develop a full multichannel spin model in momentum space to investigate three-body recombination of identical alkali-metal atoms colliding in a magnetic field. The model combines the exact three-atom spin structure and realistic pairwise atom-atom interactions. By neglecting the interaction between two particles when the spectating particle is not in its initial spin state we arrive at an approximate model. With this approximate model we achieve excellent agreement with the recent precise measurement of the ground Efimov resonance position in potassium-39 close to 33.58 G [Chapurin *et al.*, Phys. Rev. Lett. **123**, 233402 (2019)]. We analyze the limitations of our approximation by comparing to the numerical results for the full system and find that it breaks down for Feshbach resonances at larger magnetic fields in the same spin channel. There the relevant three-body closed channel thresholds are much closer to the open channel threshold, which enhances the corresponding multichannel couplings. Therefore the neglected components of the interaction should be included for those Feshbach resonances.

PACS numbers: 31.15.-p, 34.50.-s, 67.85.-d

I. INTRODUCTION

The Efimov effect describes a three-body scenario with an infinite number of loosely bound trimer states. Those bound states commonly referred to as Efimov trimers appear when the two-body interaction is tuned to be resonant and the s -wave scattering length a goes through a pole. The binding energies of these trimers follow a universal scaling relation, $E_{n+1}/E_n = e^{-2\pi/s_0}$ with $s_0 \approx 1.00624$ for identical bosons [1, 2]. This universal scaling law transfers also to other three-body observables such as the values of the scattering length at which the Efimov trimers meet the three-body continuum [2] and cause Efimov resonances in the three-body recombination rate. Conventionally, the value in scattering length related to the ground Efimov trimer resonance is defined as the three-body parameter a_- . It can be experimentally determined by measuring the three-body recombination rate as a function of the scattering length. This has been done in a variety of alkali-metal atomic gases [3–10] since the pioneering experimental work in Innsbruck [3].

Originally thought to be a free parameter, most early experimental observations [3, 5, 6, 8–10] indicated little variation of a_-/r_{vdW} over different Feshbach resonances, spin states and species, with r_{vdW} [11] the van der Waals length of the species considered. Subsequently, a theoretical study [12] based on an adiabatic hyperspherical approach explained that a_- is fixed at approximately $-9.7 r_{\text{vdW}}$

due to a universal effective three-body potential barrier that arises from pairwise van der Waals interactions. These unexpected experimental findings in combination with the successful theoretical explanations [12–14], are referred to as the van der Waals universality of the three-body parameter (TBP). This universality is believed to break down away from the broad Feshbach resonance limit, as the explanation is based on a single-channel approximation that cannot correctly describe the two-body physics of a narrow Feshbach resonance. Previous theoretical investigations based on simplified multichannel models at the two-body level [15–17] revealed a completely different behavior of a_- in the limit of narrow Feshbach resonances, indicating the importance of multichannel effects. A precise measurement in the ^{39}K gas in the vicinity of a Feshbach resonance with intermediate width has reported a violation of the single channel van der Waals universality [18]. This finding motivates our current work for developing a full multichannel spin model for three-body recombination.

Moreover, recent experimental progress has been made in the field of ultracold chemistry in a regime where the interaction is non-resonant [19–21]. These experiments focus on the distribution of three-body recombination products in ^{87}Rb . There the recombination into shallow dimers could be well explained by a single-channel model. However, the multichannel structure is required to describe recombination into deeply bound dimer states.

Multichannel effects are inherent in the three-body calculation for a system of ultracold alkali-metal atoms exposed to a magnetic field. They are neglected in most calculations due to the intractable complications of solving the three-body equations in that case. Multichannel three-body calculations

* These authors contributed equally and share first authorship.

can be performed by replacing the van der Waals interactions between the atoms with contact or separable interactions [15–17, 22–26]. However, such simplifications lead to a low accuracy, which limits the capacity of the corresponding models to analyze multichannel effects especially in view of van der Waals interactions. So far a number of numerical multichannel models including van der Waals interaction potentials have been developed [18, 27–29]. However, these models always limit the spin space of the atoms.

In this work, we supplement our three-body multichannel calculation with both the complete realistic spin structure and van der Waals pairwise interactions. This allows us to investigate three-body multichannel effects that have not been included in previous studies on a high accuracy level. The paper is organized as follows: Section II A introduces the multichannel Hamiltonian of three atoms in a magnetic field. Section II B reviews the Alt-Grassberger-Sandhas (AGS) equation and its connection to the three-body recombination rate in the multichannel case. Our numerical results for the recombination rate of three ^{39}K atoms are shown in Section III, followed by conclusions in Section IV.

II. THEORY

A. The multichannel three-body Hamiltonian

We consider a system of three identical bosonic alkali-metal atoms, where each atom i ($i = 1, 2, 3$) can occupy several internal spin states $|c_i\rangle$ with energies E_{c_i} , accounting for different hyperfine states of the electronic ground configuration [11, 30]. These spin states and energies are the eigenstates and eigenvalues of the sum of hyperfine and Zeeman terms, and can be shifted by applying an external magnetic field. The eigenstates are commonly labeled by the quantum numbers $(f, m_f) \equiv c$ that they correspond to at low magnetic field, with $\mathbf{f} = \mathbf{s} + \mathbf{i}$ the sum of the electronic \mathbf{s} and nuclear spin \mathbf{i} [11, 30]. In the limit of infinite separation the interaction between the atoms vanishes and we get the free Hamiltonian

$$H_0 = \sum_{c_1 c_2 c_3} (T + E_{c_1} + E_{c_2} + E_{c_3}) |c_1 c_2 c_3\rangle \langle c_1 c_2 c_3|, \quad (1)$$

with T the kinetic energy operator in the center of mass frame. However, when the atoms approach each other, the different spin channels $|c_1 c_2 c_3\rangle$ get coupled by a multichannel interaction potential V . When one atom k is infinitely far separated from the

other two atoms i and j , the interaction of the pair (ij) can be accurately described by model potentials V_{ij} with a long-range $-C_6/r_{ij}^6$ van der Waals tail attached to a short-range part, that depends on the nature of the combined electronic spin of atoms i and j . Here r_{ij} is the distance between atoms i and j and we note that we will sometimes use the notation $\alpha = (ij)$ to indicate a certain partition of the three atoms into a pair (ij) and the remaining particle k . When all three atoms (ijk) approach each other, the interaction needs to be adjusted by a genuine short-range three-body potential V_{ijk} . However, it has been demonstrated that V_{ijk} plays only a minor role in low energy three-body collision processes [27, 31] and is therefore often neglected. We thus take

$$V \approx \sum_{\substack{i,j=1 \\ i < j}}^3 V_{ij} \quad (2)$$

as an approximation for V . We model the multichannel pairwise interaction as a sum of singlet V_{ij}^S and triplet V_{ij}^T potentials,

$$V_{ij}(r_{ij}) = V_{ij}^S(r_{ij})\mathcal{P}_{ij}^S + V_{ij}^T(r_{ij})\mathcal{P}_{ij}^T, \quad (3)$$

according to the electronic state structure of two alkali-metal atoms. \mathcal{P}^S and \mathcal{P}^T denote the projectors on electronic singlet and triplet states, respectively. For V_{ij}^S or V_{ij}^T we take either Lennard-Jones model potentials with N and $N - 1$ s -wave bound states, respectively, as done in [18], or we take the highly accurate interaction potentials for ^{39}K as presented in [32]. Since each constituent V_{ij} conserves $M_{ij}^{2b} = m_{fi} + m_{fj}$, $M^{3b} = m_{f1} + m_{f2} + m_{f3}$ is a good quantum number of the system under the interaction of Eq. (2). A Full Multichannel Spin (FMS) model in this situation needs to consider all spin channels $\{|c_1 c_2 c_3\rangle | M^{3b} = M_{\text{in}}^{3b}\}$ that have the same M^{3b} as the incoming spin state M_{in}^{3b} . Some typical examples of the spin channel energies involved in a three-body collision with $M^{3b} = -3$ for ^{39}K can be found in Fig. 1(a). We note that even for a system of three identical bosons even and odd parity dimer channels couple in the multichannel scenario, which contrasts with the single channel case where such a coupling is absent. This coupling has been observed experimentally [19].

We also analyze a simplified approximate model, which we refer to as the Fixed Spectating Spin (FSS) model. For that we restrict the pairwise interaction V_{ij} to the incoming spin component $|c_k^{\text{in}}\rangle$ of the spectating atom and thereby set the interaction to zero in cases where the spin of the spectating atom is not in the incoming component,

$$V_{ij}^{\text{FSS}}(r_{ij}) = V_{ij}(r_{ij}) |c_k^{\text{in}}\rangle \langle c_k^{\text{in}}|. \quad (4)$$

In that way only parts of the interaction potential are neglected while the spin structure is kept intact. This approximation is valid when the incoming channel is the only open channel and not all three atoms can get in close proximity to each other simultaneously. In the single-channel scenario it has been demonstrated that a repulsive barrier that arises in the effective three-body potential of the Efimov channel prevents all three atoms being close. Consequently, the restriction of Eq. (4) is a natural choice when the full multichannel three-body problem is too complicated to solve. Similar restrictions on the spectating atom's spin are implemented in most previous proposals [18, 27, 28, 33], however in all those models the natural three-body spin structure is also altered or further restricted in course of the approximation. In the AGS equation below this leads to a transition operator between atoms i and j that projects onto $|c_k^{\text{in}}\rangle$ and consequently we could as well restrict the complete AGS equation to $c_k = c_k^{\text{in}}$.

B. Three-body recombination

Following Ref. [31, 34–36], one can obtain the three-body recombination rate

$$K_3(E) = \frac{24\pi m}{\hbar} (2\pi\hbar)^6 \sum_{d,c_d} q_d |\alpha\langle (q_d, c_d), \varphi_d | U_{\alpha 0}(z) | \psi_{\text{in}} \rangle|^2 \quad (5)$$

by evaluating the transition operator element $\alpha\langle (q_d, c_d), \varphi_d | U_{\alpha 0}(z) | \psi_{\text{in}} \rangle$, from a free incoming state ψ_{in} of energy E into a α -dimer d with wave function φ_d and energy E_d plus a free atom of spin c_d and absolute momentum q_d relative to the dimer center-of-mass, on the energy shell. This leads to $E = 3q_d^2/4m + E_{c_d} + E_d$ and the complex energy $z = E + i0$, which means that we take the limit in z from the upper half of the complex energy plane. Here m denotes the mass of a single atom.

The transition operator $U_{\alpha 0}(z)$ related to three-body recombination into the α -dimer state is defined by the AGS equation for three identical bosons [26, 31, 36, 37]

$$U_{\alpha 0}(z) = \frac{1}{3} G_0^{-1}(z) [1 + P_+ + P_-] + [P_+ + P_-] \mathcal{T}_\alpha(z) G_0(z) U_{\alpha 0}(z). \quad (6)$$

The operators G_0 and \mathcal{T}_α denote the free Greens operator and a generalized two-body transition operator, respectively. The operators P_+ and P_- are the cyclic and anticyclic permutation operators, respectively, that act on both coordinates and spins, since

in a situation with realistic spin structure which we are considering in this work all operators in the AGS equation need to be generalized to account for the multichannel spin structure. The three-body free Greens operator G_0 includes the shifts in the thresholds in different three-body spin channels

$$G_0(z) = (z - H_0)^{-1} = \sum_{c_1, c_2, c_3} \frac{|c_1 c_2 c_3\rangle \langle c_1 c_2 c_3|}{z - E_{c_1} - E_{c_2} - E_{c_3} - T}. \quad (7)$$

From Equation (7) we can infer, that G_0 can serve as a suppressing factor in channels with large threshold difference to the incoming channel $\Delta E = \sum_{i=1}^3 (E_{c_i} - E_{c_i^{\text{in}}}) \gg E_{\text{vdW}}$ in the low energy and low momentum regime where both $z - \sum_{i=1}^3 E_{c_i^{\text{in}}}$ and T are small. Here $E_{\text{vdW}} = \hbar^2/mr_{\text{vdW}}^2$ is the van der Waals energy. We interpret our numerical three-body results close to Feshbach resonances with varying threshold differences in view of the suppressing properties of ΔE in section III. The generalized two-body transition operator \mathcal{T}_α is given by

$$\mathcal{T}_\alpha(z) = (1 - V_\alpha G_0(z))^{-1} V_\alpha = \sum_{c_k} \int d\mathbf{q} t(z - E_{c_k} - \frac{3q^2}{4m}) |c_k, \mathbf{q}\rangle_{\alpha\alpha} \langle c_k, \mathbf{q}|, \quad (8)$$

where $t(z - E_{c_k} - 3q^2/4m)$ is the two-body transition operator acting on the spin and relative coordinate of the pair of atoms (ij). The relative momentum between the center of mass of the pair (ij) and the atom k is denoted by \mathbf{q} . The partial wave components of $t(z - E_{c_k} - 3q^2/4m)$ can be obtained by extending the method in Ref. [36] to the multichannel case. In the following we will omit the explicit dependence on z for notational compactness unless it is needed.

In the on-shell limit $z = E + i0$, it is more convenient to define a new operator A_α [36]

$$A_\alpha = 3G_0 (P_+ + P_-) \mathcal{T}_\alpha G_0 U_{\alpha 0}, \quad (9)$$

which fulfills the following equation

$$A_\alpha = G_0 (P_+ + P_-) \mathcal{T}_\alpha [1 + P_+ + P_- + A_\alpha]. \quad (10)$$

as a consequence of Eq. (6). Since the inhomogeneous term in $U_{\alpha 0}$ evaluates to zero when applied on $|\psi_{\text{in}}\rangle$, we get

$$\alpha\langle (q_d, c_d), \varphi_d | U_{\alpha 0}(z) | \psi_{\text{in}} \rangle = \frac{1}{3} \alpha\langle (q_d, c_d), \varphi_d | V_\alpha A_\alpha | \psi_{\text{in}} \rangle \quad (11)$$

in the on-shell limit (see Ref. [36] for more details), so that we can consider Eq. (10) instead of Eq. (6) to obtain K_3 .

We expand $\mathcal{T}_\alpha = \int dq q^2 \sum_i \tau_\alpha(i, q) |i, q\rangle_\alpha \langle i, q|$ and use the incoming state $|\psi_{\text{in}}\rangle$, such that we arrive at the linear system

$$\begin{aligned} & {}_\alpha \langle q', i' | A_\alpha | \psi_{\text{in}} \rangle \\ &= \int dq q^2 \sum_i \langle q', i' | G_0 (P_+ + P_-) | q, i \rangle_\alpha \tau_\alpha(q, i) \\ & \quad [{}_\alpha \langle q, i | (1 + P_+ + P_-) | \psi_{\text{in}} \rangle + {}_\alpha \langle q, i | A_\alpha | \psi_{\text{in}} \rangle]. \end{aligned} \quad (12)$$

The partial three-body recombination rates are then obtained by evaluating the on-shell elements of ${}_\alpha \langle q, i | A_\alpha | \psi_{\text{in}} \rangle$, since the expansion base ${}_\alpha \langle q, i |$ naturally includes the terms ${}_\alpha \langle (q_d, c_d), \varphi_d | V_\alpha$. It should be noted that the multichannel structure of Eq. (12) is implicitly contained in all operators and state vectors. Therefore Eq. (12) is a multichannel generalization of the corresponding equation in Ref. [36] even though both look identical. More details on the linear system can be found in appendix A.

III. RESULTS

Recently, three-body recombination rates were precisely measured in a ^{39}K atomic gas near a Feshbach resonance at 33.58 G. The three-body parameters a_- and η , characterizing the position and width of the lowest Efimov resonance, are extracted and confirmed by a state-of-the-art adiabatic hyperspherical calculation [18]. The measurement was found to be in agreement with a previous experimental result [38]. This poses ideal circumstances for checking our new numerical method. For that we have to consider a system of three ^{39}K atoms initially prepared in the $|f_1 = 1, m_{f_1} = -1\rangle |f_2 = 1, m_{f_2} = -1\rangle |f_3 = 1, m_{f_3} = -1\rangle$ state in an external magnetic field B .

We first use the FSS model to obtain the position a_- and width η of the lowest Efimov resonance of three ^{39}K atoms nearby $B = 33.58$ G. For that, we calculate the three-body recombination rate $K_3(0)$ by solving Eq. (12) at zero energy for a set of magnetic fields close to the lowest Efimov resonance and fit the universal expressions for $K_3(0)$ [2] to our results. In our numerical computations, we restrict to a maximum of $\ell_{\text{max}} = 10$ partial waves in the atom-dimer momentum and to an integration range in q of $[0, q_{\text{max}}]$. We implement $q_{\text{max}} = 20 \hbar/r_{\text{vdW}}$ in our calculations if not specified differently. We optimize the parameters of our Lennard-Jones potential model to best represent the two-body scattering length a in the $M_{ij}^{2b} = -2$ channel close to the Feshbach profile with magnetic field points being sampled in both background and resonance regimes.

Table I shows our results for Lennard-Jones potentials with N singlet s -wave dimer states and for the realistic molecular potentials including Born-Oppenheimer corrections from Ref. [32]. For the Lennard-Jones potential our results show just little variation of a_- when the number of s -wave dimers supported by the singlet potential is changed from $N = 2$ to $N = 5$, in contrast to the constant decrease of a_- that has been found for the model in Ref. [18]. Qualitatively, the behavior we find is more similar to that of a single channel model [12]. When using the realistic molecular potentials, we find $a_- \approx -14 r_{\text{vdW}}$, in excellent agreement with the experimental result $a_- = -14.05(17) r_{\text{vdW}}$.

We find that $\ell_{\text{max}} = 10$ is sufficient for a good convergence in the FSS model, as can be seen from the ℓ_{max} -dependence of the FSS model results presented in Table II. The error resulting from the restriction in integration range has been analyzed for single channel Lennard-Jones potentials with close to 4 and 6 bound s -wave dimer states [36]. There the error in a_- is demonstrated to be 2 % for $q_{\text{max}} = 20 \hbar/r_{\text{vdW}}$ and 0.5 % for $q_{\text{max}} = 40 \hbar/r_{\text{vdW}}$. We estimate that the error from restricting the integration range is of similar order of magnitude in our present calculations. In this view, our results for a_- are reliable up to uncertainties of a few percent. The error in η , however, could be large according to our analysis in [36].

To go beyond the FSS approximation, we consider the FMS model of the three atom system. For the $N = 2$ Lennard-Jones potentials representing the Feshbach resonances at 33.58 G in the $M_{ij}^{2b} = -2$ channel, we perform the calculation in the FMS model and find a_- in good agreement with the FSS results (see Table II), indicating that the FSS model is a good approximation when considering a_- .

However, considering the Feshbach resonances at larger magnetic fields of 162.35 and 560.72 G in the $M_{ij}^{2b} = -2$ channel represented by $N = 2$ Lennard-Jones potentials we find that the FSS approximation is breaking down. That is apparent by comparing the FSS and FMS results in Table III. A possible reason for this could be that the spin states neglected in the FSS model are less suppressed in these cases. A suppression in the coupling to those spin channels arises due to the separation in channel energy, which we commented on after Eq. (7). As is depicted in Figs. 1(a) and 1(b) this separation is much larger for the resonance at 33.58 G (FR1) than for the one at 162.35 (FR2) and 560.72 G (FR3). Therefore we suspect that the FSS model works for the FR1 but the FMS model has to be used for FR2 and FR3.

Even though our $N = 2$ Lennard-Jones FMS results are not completely converged for FR2 and FR3, they tend to be in disagreement with the experi-

TABLE I. Comparison of three-body parameters from Ref. [18] and our FSS calculation (this work) with Lennard-Jones (LJ) potentials supporting different number N of singlet s -wave dimer states. Our results with realistic ^{39}K molecular potentials (full) and the experimental measurement [18] are also shown. A momentum cutoff at $q_{\max} = 20 \hbar/r_{\text{vdW}}$ is implemented in all calculations in this work except for the ‘full40’ case, where $q_{\max} = 40 \hbar/r_{\text{vdW}}$ instead. For definiteness, the singlet and triplet scattering lengths specifying the potentials we use are listed in the last two columns.

	$a_- [r_{\text{vdW}}]$		η		$a^S [r_{\text{vdW}}]$	$a^T [r_{\text{vdW}}]$
	this work	Ref. [18]	this work	Ref. [18]		
$N=2$, LJ	-13.51	-7.61	0.23	0.10	1.3503	-0.5098
$N=3$, LJ	-14.33	-11.20	0.20	0.19	1.7281	-0.5238
$N=4$, LJ	-14.16	-12.27	0.18	0.20	1.8479	-0.5238
$N=5$, LJ	-14.60	-12.69	0.20	0.21	1.9036	-0.5238
full	-14.12	-	0.15	-	2.1432	-0.5181
full40	-14.03	-	0.19	-	2.1432	-0.5181
measurement	-14.05 (17)		0.25 (1)			

TABLE II. Comparison of three-body parameters from the FSS and FMS calculations with $N = 2$ Lennard-Jones potentials concentrating on the same Feshbach resonance as in Table I. ℓ_{\max} denotes the maximum dimer partial-wave included in the calculation. The FSS result with realistic molecular potential and $q_{\max} = 40/r_{\text{vdW}}$ (full40) is also shown.

ℓ_{\max}	FSS ($N = 2$, LJ)		FMS ($N = 2$, LJ)		FSS (full40)	
	$a_- [r_{\text{vdW}}]$	η	$a_- [r_{\text{vdW}}]$	η	$a_- [r_{\text{vdW}}]$	η
0	-14.19	0.14	-18.34	0.17	-14.52	0.16
2	-15.73	0.17	-20.66	0.06	-15.34	0.15
4	-13.90	0.20	-14.32	0.15	-14.89	0.19
6	-13.60	0.23	-13.50	0.20	-14.42	0.18
8	-13.55	0.23	-13.37	0.19	-14.25	0.19
10	-13.51	0.23	-	-	-14.03	0.19

TABLE III. Three-body parameters from FSS and FMS calculation with $N = 2$ Lennard-Jones or realistic ^{39}K molecular potential (full). The upper and lower panels list the results for FR2 at 162.35 G and FR3 at 560.72 G, respectively.

ℓ_{\max}	FSS ($N = 2$, LJ)		FMS ($N = 2$, LJ)		FMS (full)	
	$a_- [r_{\text{vdW}}]$	η	$a_- [r_{\text{vdW}}]$	η	$a_- [r_{\text{vdW}}]$	η
0	-31.22	0.12	-24.34	0.11	-29.74	0.16
2	-32.68	0.40	-9.83	0.29	-27.29	0.20
4	-35.70	0.57	-38.48	0.29	-25.05	0.20
6	-33.85	0.53	-29.23	0.33	-24.33	0.21
8	-33.79	0.54	-27.53	0.33	-24.14	0.22
10	-33.81	0.54	-	-	-	-
0	-18.91	0.16	-19.07	0.06	-27.17	0.14
2	-16.73	0.02	-11.30	0.26	-19.32	0.13
4	-15.42	0.03	-24.14	0.71	-15.93	0.06
6	-15.00	0.04	-19.28	0.47	-14.76	0.09
8	-14.85	0.04	-18.54	0.45	-13.98	0.11
10	-14.78	0.04	-	-	-	-

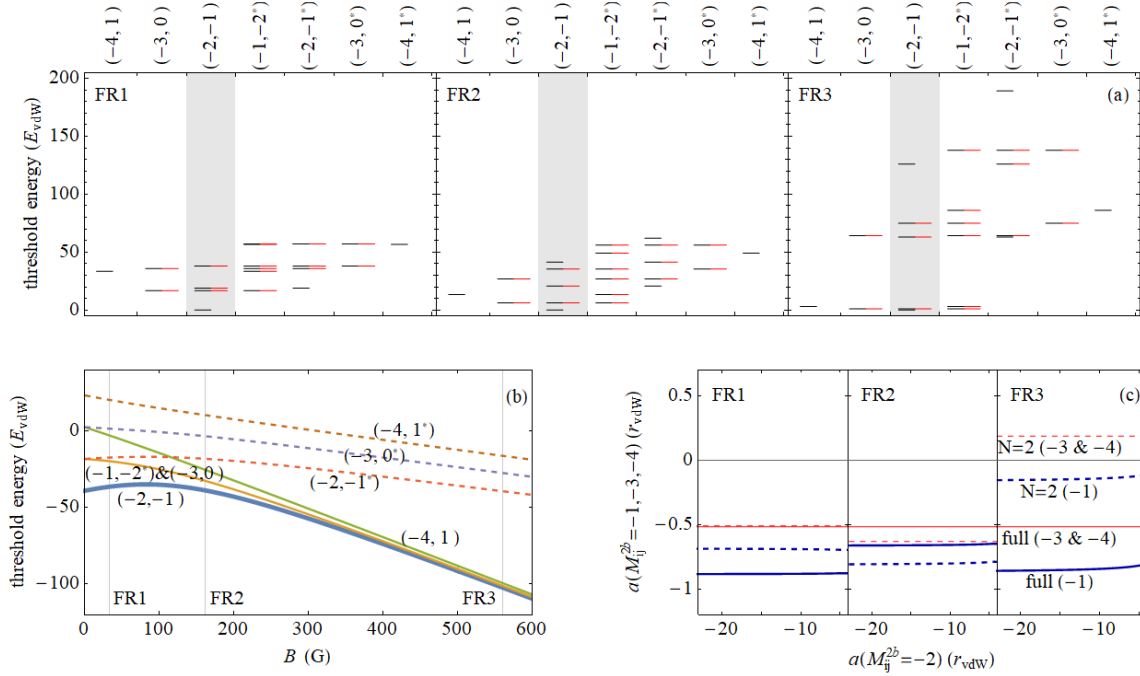


FIG. 1. (a) Threshold energies relative to the incoming channel of all spin channels involved in the FMS model for the different Feshbach resonances analyzed. The spin channels are grouped by the quantum numbers (M_{ij}^{2b}, m_{fk}) along the x -direction. The m_{fk} and m_{fk}^* correspond to the $|f_k = 1, m_{fk}\rangle$ and $|f_k = 2, m_{fk}\rangle$ states, respectively and we distinguish thresholds related to even and odd parity by black and red coloring, respectively. We note that threshold lines with the same x -position are directly coupled by V_α . The gray shaded area indicates the thresholds that are included in the FSS model. (b) Lowest threshold energies with (M_{ij}^{2b}, m_{fk}) involved in the colliding system of three ^{39}K atoms with $M^{3b} = -3$. The vertical gray lines denote the Feshbach Resonance at 33.58 G (FR1), 162.35 G (FR2) and 560.72 G (FR3). (c) Two-body scattering length with different M_{ij}^{2b} as a function of the incoming channel two-body scattering length $a(M_{ij}^{2b} = -2)$ from the fitted ($N = 2$) Lennard-Jones potentials (dashed) and realistic molecular potentials (full). For three-body calculations with $M^{3b} = -3$ the two-atom spin states involved have $M_{ij}^{2b} = -1, -3, -4$.

mental observations of $a_- = -11.3(1.9) r_{\text{vdW}}$ for FR2 and $a_- = -9.9(1.4) r_{\text{vdW}}$ for FR3 [38]. A reason could be that the pairwise interactions in the two-body channels with $M_{ij}^{2b} = -1, -3$ and -4 are not accurately represented. Since the Lennard-Jones potentials are just adjusted to represent the interactions in the $M_{ij}^{2b} = -2$ channel correctly, it is not surprising that the interactions in the other two-body channels deviate from the original interactions. This can be seen when comparing the corresponding two-body scattering lengths shown in Fig. 1(c), in which we find deviations for all three cases. The deviations in case of FR1 are not causing problems since the contribution from the inaccurately represented interactions can be neglected.

We also give the FMS results for the realistic molecular potentials in Table III, even though they are not converged in the partial waves included. The results including up to 8 partial waves already indicate a better agreement with the experimental results for the resonances at 162.75 and 560.72 G than the Lennard-Jones potential model. We note that for the realistic potentials the interactions in all spin states are correctly represented.

IV. CONCLUSION AND OUTLOOK

In summary, we study multichannel effects on three-body recombination of ultracold ^{39}K atoms. We solve the three-body equation with van der Waals pairwise interactions including the realistic spin structure of the system. We numerically confirm that restricting the pairwise interaction to the incoming spin component of the spectating atom, i.e. the FSS model, is a good approximation around the Feshbach resonance at 33.58 G in the $M_{ij}^{2b} = -2$ channel. The FSS model gives $a_- \approx -14 r_{\text{vdW}}$ in excellent agreement with the current precise measurement $a_- = -14.05(17) r_{\text{vdW}}$ [18]. In addition, we analyzed the limitations of the FSS model by investigating two other Feshbach resonances at 162.35 and 560.72 G. There the three-body channels neglected in the FSS model are less suppressed due to the smaller threshold difference to the open channel and need to be taken into account. In such a situation, the interactions in all contributing channels should be well represented to arrive at an accurate full multichannel spin model.

The results of this work raise doubts on the approximation of restricting or altering the realistic three-atom spin structure, which has been implemented earlier to enable multichannel three-body numerical calculations [18, 27, 28, 33]. To determine in which situations this approximation is valid and when it is not is an important task, which needs to be

further clarified in future investigations. Nonetheless, we gained some preliminary insight. At large threshold differences, three-body multichannel couplings to the neglected channels can be suppressed. This could be one indicator for the regime in which the approximation holds. In this view, it can be expected that heavier species, such as Rb and Cs for which the threshold differences relative to the van der Waals energy scale are generally larger, are better represented by the approximation than lighter ones, such as Na and Li. This may explain that agreement has been achieved with multichannel models for Rb and Cs systems [27], but not for the Li system. In addition, the strength of the two-body multichannel coupling which is related to the width parameter s_{res} [11] of a Feshbach resonance, may also affect the validity of the approximation. A more rigorous treatment should take both the threshold difference and s_{res} into account.

ACKNOWLEDGEMENTS

We thank José D’Incao, Denise Ahmed-Braun, Victor Colussi, Gijs Groeneveld, and Silvia Musolino for discussions. This research is financially supported by the Netherlands Organisation for Scientific Research (NWO) under Grant No. 680-47-623.

Appendix A: Details for solving Eq. (12)

In order to solve Eq. (12), one needs to evaluate $\langle q', i' | G_0(P_+ + P_-) | q, i \rangle_\alpha$ and ${}_\alpha \langle q, i | (1 + P_+ + P_-) | \psi_{\text{in}} \rangle$, which requests $|q, i\rangle_\alpha$ at first. We note that $|q, i\rangle_\alpha$ is a multichannel analogue as that in Ref. [36] and can be calculated by the same mapped grid Hamiltonian approach [39]. To be explicit,

$$|i\rangle = \sum_C |\chi(p; C, n, q, c_k, \Lambda)\rangle |C\rangle |c_k\rangle |\Lambda\rangle, \quad (\text{A1})$$

where $|\Lambda\rangle = |L\ell JM_J\rangle$ denote quantum numbers for all spatial angular momenta, say, L for the atom-dimer orbit, ℓ for the dimer orbit, J and M_J for the total orbit. $|C\rangle$ describes the spin state $|c_i c_j\rangle$ of pair (i, j) , which is chosen to be symmetric for even ℓ and antisymmetric for odd ℓ considering the identical bosonic system in this work. Note that the summation over C is under the restriction of $M_{ij}^{2b} + m_{f_k} = M^{3b}$. $|\chi(p; C, n, q, c_k, \Lambda)\rangle$ is the C channel component of n th eigenstate of two-body ℓ th partial-wave transition operator, which is obtained at $E^{2b} = E - E_{c_k} - 3q^2/4m$. In terms of the two-body spin basis $|C\rangle$, it can be proved that P_+ and P_- contribute equally in Eq. (12) as is done in Ref. [40]. In the following, we shall replace $P_+ + P_-$ by

$2P_+$ in $\langle q', i' | G_0(P_+ + P_-) | q, i \rangle_\alpha$ and ${}_\alpha \langle q, i | (1 + P_+ + P_-) | \psi_{\text{in}} \rangle$.

The zero energy incoming state can be written as

$$| \psi_{\text{in}} \rangle = | q = 0, p = 0, C^{\text{in}}, c_k^{\text{in}}, \Lambda = 0 \rangle, \quad (\text{A2})$$

where $\Lambda = 0$ means $L = 0, \ell = 0, J = 0$ and $M_J = 0$. So that ${}_\alpha \langle q, i | (1 + P_+ + P_-) | \psi_{\text{in}} \rangle$ is given by

$$\begin{aligned} {}_\alpha \langle q, i | (1 + 2P_+) | \psi_{\text{in}} \rangle &= \sum_C \chi(0; C, n, 0, c_k^{\text{in}}, 0) \\ &\times \frac{\delta(q)}{q^2} \langle C c_k | (1 + 2P_+^s) | C^{\text{in}} c_k^{\text{in}} \rangle \delta_{\Lambda 0}, \end{aligned} \quad (\text{A3})$$

where P_+^s is P_+ acting on spin space. $\langle q', i' | G_0(P_+ + P_-) | q, i \rangle_\alpha$ is more complicated, which consists of a lot inner products of $\langle \chi', C', n', q', c'_k, \Lambda' | G_0 P_+ | \chi, C, n, q, c_k, \Lambda \rangle$ according to Eq. (A1). Due to the conservation of total angular momentum of three atoms, we have $|\Lambda\rangle = |\ell, \ell, 0, 0\rangle$ and then get

$$\begin{aligned} &\langle \chi', C', n', q', c'_k, \Lambda' | G_0 P_+ | \chi, C, n, q, c_k, \Lambda \rangle \\ &= \langle \chi', n', q', \Lambda' | \hat{G}_0 (E - E_C - E_{c_k}) \hat{P}_+^c | \chi, n, q, \Lambda \rangle \langle C' c'_k | (P_+^s) | C c_k \rangle \\ &= \frac{(-1)^\ell \sqrt{2\ell' + 1} \sqrt{2\ell + 1}}{2} \int_{-1}^1 du P_{\ell'} \left(\frac{q'^2/2 + q'qu}{q' \sqrt{q'^2/4 + q^2 + q'qu}} \right) P_\ell \left(\frac{q^2/2 + q'qu}{q \sqrt{q^2/4 + q'^2 + q'qu}} \right) \\ &\times \frac{\left[\chi(\sqrt{q'^2/4 + q^2 + q'qu}; C', q', n', c'_k, \Lambda') \right]^* \chi(\sqrt{q^2/4 + q'^2 + q'qu}, C, n, q, c_k, \Lambda)}{E + i0 - E_C - E_{c_k} - q'^2/m - q^2/m - q'qu/m} \langle C' c'_k | (P_+^s) | C c_k \rangle, \end{aligned} \quad (\text{A4})$$

where P_+^c is P_+ acting on coordinate space and P_ℓ

the Legendre polynomial.

-
- [1] V. Efimov, *Physics Letters B* **33**, 563 (1970).
[2] E. Braaten and H.-W. Hammer, *Physics Reports* **428**, 259 (2006).
[3] T. Kraemer, M. Mark, P. Waldburger, J. Danzl, C. Chin, B. Engeser, K. Pilch, A. Jaakkola, H.-C. Nägerl, and R. Grimm, *Nature* **440**, 315 (2006).
[4] S. E. Pollack, D. Dries, and R. G. Hulet, *Science* **326**, 1683 (2009).
[5] N. Gross, Z. Shotan, S. Kokkelmans, and L. Khaykovich, *Phys. Rev. Lett.* **103**, 163202 (2009).
[6] N. Gross, Z. Shotan, S. Kokkelmans, and L. Khaykovich, *Phys. Rev. Lett.* **105**, 103203 (2010).
[7] M. Zaccanti, B. Deissler, C. D'Errico, M. Fattori, M. Jona-Lasinio, S. Müller, G. Roati, M. Inguscio, and G. Modugno, *Nature Physics* **5**, 586 (2009).
[8] R. J. Wild, P. Makotyn, J. M. Pino, E. A. Cornell, and D. S. Jin, *Phys. Rev. Lett.* **108**, 145305 (2012).
[9] F. Ferlaino, A. Zenesini, M. Berninger, B. Huang, H.-C. Nägerl, and R. Grimm, *Few-Body Systems* **51**, 113 (2011).
[10] M. Berninger, A. Zenesini, B. Huang, W. Harm, H.-C. Nägerl, F. Ferlaino, R. Grimm, P. S. Julienne, and J. M. Hutson, *Phys. Rev. Lett.* **107**, 120401 (2011).
[11] C. Chin, R. Grimm, P. Julienne, and E. Tiesinga, *Rev. Mod. Phys.* **82**, 1225 (2010).
[12] J. Wang, J. P. D'Incao, B. D. Esry, and C. H. Greene, *Phys. Rev. Lett.* **108**, 263001 (2012).
[13] P. Naidon, S. Endo, and M. Ueda, *Phys. Rev. A* **90**, 022106 (2014).
[14] P. Naidon, S. Endo, and M. Ueda, *Phys. Rev. Lett.* **112**, 105301 (2014).
[15] D. S. Petrov, *Phys. Rev. Lett.* **93**, 143201 (2004).
[16] A. O. Gogolin, C. Mora, and R. Egger, *Phys. Rev. Lett.* **100**, 140404 (2008).
[17] R. Schmidt, S. P. Rath, and W. Zwerger, *The European Physical Journal B* **85**, 386 (2012).
[18] R. Chapurin, X. Xie, M. J. Van de Graaff, J. S. Popowski, J. P. D'Incao, P. S. Julienne, J. Ye, and E. A. Cornell, *Phys. Rev. Lett.* **123**, 233402 (2019).
[19] A. Härter, A. Krüchow, M. Deiß, B. Drews, E. Tiemann, and J. H. Denschlag, *Nature Physics* **9**, 512 (2013).
[20] J. Wolf, M. Deiß, A. Krüchow, E. Tiemann, B. P. Ruzic, Y. Wang, J. P. D'Incao, P. S. Julienne, and J. H. Denschlag, *Science* **358**, 921 (2017).
[21] J. Wolf, M. Deiß, and J. Hecker Denschlag, *Phys. Rev. Lett.* **123**, 253401 (2019).
[22] P. Massignan and H. T. C. Stoof, *Phys. Rev. A* **78**, 030701 (2008).
[23] P. Naidon and M. Ueda, *Comptes Rendus Physique* **12**, 13 (2011), few body problem.
[24] V. E. Colussi, C. H. Greene, and J. P. D'Incao, *Phys. Rev. Lett.* **113**, 045302 (2014).

- [25] J.-L. Li and S.-L. Cong, *Phys. Rev. A* **99**, 022708 (2019).
- [26] T. Secker, D. J. M. Ahmed-Braun, P. M. A. Mestrom, and S. J. J. M. F. Kokkelmans, to be published.
- [27] Y. Wang and P. S. Julienne, *Nature Physics* **10**, 768 (2014).
- [28] K. Kato, Y. Wang, J. Kobayashi, P. S. Julienne, and S. Inouye, *Phys. Rev. Lett.* **118**, 163401 (2017).
- [29] X. Xie, M. J. V. de Graaff, R. Chapurin, M. D. Frye, J. M. Hutson, J. P. D’Incao, P. S. Julienne, J. Ye, and E. A. Cornell, “Observation of efimov universality across a non-universal feshbach resonance in ^{39}K ,” (2020), [arXiv:2008.00396](https://arxiv.org/abs/2008.00396).
- [30] C. J. Pethick and H. Smith, *Bose–Einstein Condensation in Dilute Gases*, 2nd ed. (Cambridge University Press, 2008).
- [31] M. D. Lee, T. Köhler, and P. S. Julienne, *Phys. Rev. A* **76**, 012720 (2007).
- [32] S. Falke, H. Knöckel, J. Friebe, M. Riedmann, E. Tiemann, and C. Lisdat, *Phys. Rev. A* **78**, 012503 (2008).
- [33] S. Jonsell, *Journal of Physics B: Atomic, Molecular and Optical Physics* **37**, S245 (2004).
- [34] A. J. Moerdijk, H. M. J. M. Boesten, and B. J. Verhaar, *Phys. Rev. A* **53**, 916 (1996).
- [35] G. Smirne, R. M. Godun, D. Cassettari, V. Boyer, C. J. Foot, T. Volz, N. Syassen, S. Dürr, G. Rempe, M. D. Lee, K. Góral, and T. Köhler, *Phys. Rev. A* **75**, 020702 (2007).
- [36] T. Secker, J. L. Li, P. M. A. Mestrom, and S. J. J. M. F. Kokkelmans, “Efficient three-body calculations with a two-body mapped grid method,” (2020), [arXiv:2011.01707](https://arxiv.org/abs/2011.01707).
- [37] P. M. A. Mestrom, T. Secker, R. M. Kroeze, and S. J. J. M. F. Kokkelmans, *Phys. Rev. A* **99**, 012702 (2019).
- [38] S. Roy, M. Landini, A. Trenkwalder, G. Semeghini, G. Spagnolli, A. Simoni, M. Fattori, M. Inguscio, and G. Modugno, *Phys. Rev. Lett.* **111**, 053202 (2013).
- [39] K. Willner, O. Dulieu, and F. Masnou-Seeuws, *The Journal of Chemical Physics* **120**, 548 (2004).
- [40] W. Glöckle, *The quantum mechanical few-body problem*, Texts and monographs in physics (Springer, Berlin, 1983).